P819

Observations of Hailstone Characteristics in Multicell and Supercell Thunderstorms

Ian M. Giammanco*, Tanya M. Brown

Insurance Institute for Business & Home Safety

INTRODUCTION

Severe hail events are responsible for nearly $1 billion dollars in annual insured property losses in the United States (Changnon et al. 2009). Despite a general negative trend in population growth across the Great Plains of the United States, an increasing trend in hail-related losses has been observed over the past decade (MunichRe 2013). The increase in property losses, has generated a renewed interest in understanding how the characteristics of hail may influence damage to existing building stock and new construction.

In 2011, the Insurance Institute for Business & Home Safety (IBHS) began a comprehensive research program focused on understanding the damage potential of hail, improving laboratory test methodologies, developing damage functions for a variety of new and aged building components, and evaluating construction practices which may help mitigate losses. A key component to this program has been a field phase in which in-situ measurements of the characteristics of hailstones are made.

MEASUREMENTS

Each hailstone was photographically cataloged in the field based on its collection location and by its associated parent thunderstorm. The dimensions of each stone were measured (x_1, y) assuming that two dimensions of the stone ($x_1 \approx x_2$) are relatively similar and larger than the third axis (y) as shown in Figure 1. Measuring these dimensions also allowed for a reasonable estimate of the cross-sectional area of the hailstone. Figure 2 provides a diagram of the measured dimensions and Figure 2 shows a sample photograph of a measured hailstone. Each stone was also weighed in the field using a digital scale.

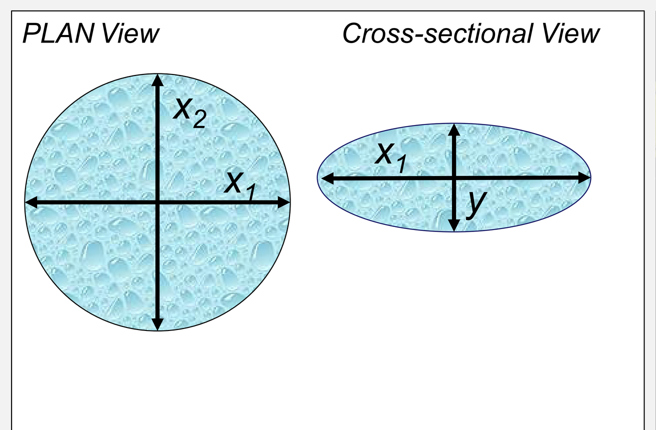

Figure 1. Diagram of measured hailstone dimensions. The x_1 and y dimensions were measured in the field.

Figure 2. Cataloged photograph from 20 May 2013 of a measured hailstone.

Hailstones are often qualitatively referred to as: "hard", "soft" or "slushy" with no quantitative means of describing the hardness of a given stone (Bilhelm and Relf, 1937; Carte 1966; Knight and Knight 1973). Brown et al. (2012) developed a unique piece of instrumentation to fill this observational gap (Figure 3). The 2012 and 2013 field campaigns provided the first opportunity to collect pilot data on the hardness of natural hailstones.

Figure 3. Compressive force test being conducted on a hailstone on 18 May 2013.

The test-device measures the applied force on a hailstone until it fractures or compresses. Figure 4 shows a time history of compressive force for three consecutive tests on three different hailstones. The rate of force applied to the stone through the device is large enough to produce a fast deformation rate and subsequent brittle failure. The measured compressive force at the point of initial fracture is used to calculate the compressive stress.

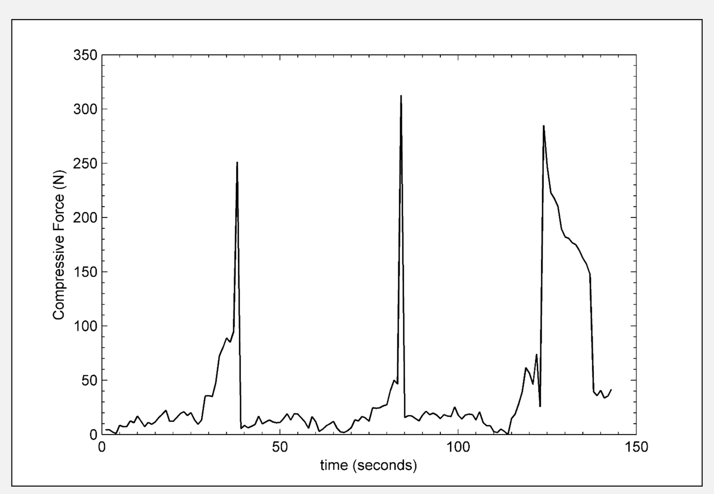

Figure 4. Time history of measured compressive force for three consecutive tests for three different hailstones from 18 May 2013.

HAIL OBSERVATIONS

The 2012-2013 dataset contains 921 hailstones measured on 14 operation days. The measurement locations for the study are shown in Figure 5. Table 1 provides a summary of each sampled event and the associated summary statistics.

Table 1. Data summary for all 2012-2013 sampled events.*indicates multiple measurement locations within the hail swath.

Case	Date	Location	Sample Size	Max Diameter (cm)	Mean Diameter (cm)	Max Compressive Stress (mPa)	Mean Compressive Stress (mPa)
1A-2012	5-27-12	Ravenna, NE	5	1.93	1.35	1.33	0.88
2A-2012	5-28-12	Lindsay, OK	32	4.75	2.77	2.21	0.89
3A-2012	5-29-12	Kingfisher, OK	20	7.75	2.31	3.71	1.24
3B-2012	5-29-12	Greenfield, OK	17	3.05	1.93	4.32	1.31
4A-2012	6-1-12	Channing, TX	45	3.12	1.80	4.20	0.85
5A-2012	6-2-12	Eads, CO	17	3.33	1.63	0.76	0.39
*6A-2012	6-6-12	Cheyenne, WY	36	3.23	1.44	0.54	0.22
7A-2012	6-7-12	LaGrange, WY	8	3.76	3.12	0.64	0.38
*7B-2012	6-7-12	LaGrange, WY	59	5.41	3.02	2.77	0.57
*1A-2013	5-17-13	Hyannis, NE	85	3.30	1.41	4.57	0.81
2A-2013	5-18-13	Paradise, KS	6	1.82	0.96	0.41	0.40
*3A-2013	5-19-13	Wichita, KS	112	3.20	1.47	4.24	0.61
3B-2013	5-19-13	Arkansas City, KS	16	3.43	1.51	1.51	0.64
*3C-2013	5-19-13	Blackwell/Newkirk, OK	23	2.51	1.11	1.51	0.55
*3D-2013	5-19-13	Cedar Vale, OK	71	3.99	2.08	1.12	0.29
3E-2013	5-19-13	Burbank, OK	18	2.21	1.11	1.80	0.95
*4A-2013	5-20-13	Antioch, OK	212	4.80	0.81	3.34	0.56
5A-2013	5-30-13	Blanchard, OK	15	3.98	2.08	1.58	0.59
*5B-2013	5-30-13	Ratliff City, OK	29	10.69	2.61	3.88	0.70
6A-2013	6-1-13	Mason, TX	29	2.99	1.60	7.46	1.64
6B-2013	6-1-13	London, TX	30	3.60	1.88	6.46	1.43
7A-2013	6-2-13	Elmwood, OK	36	3.71	1.88	2.86	0.51

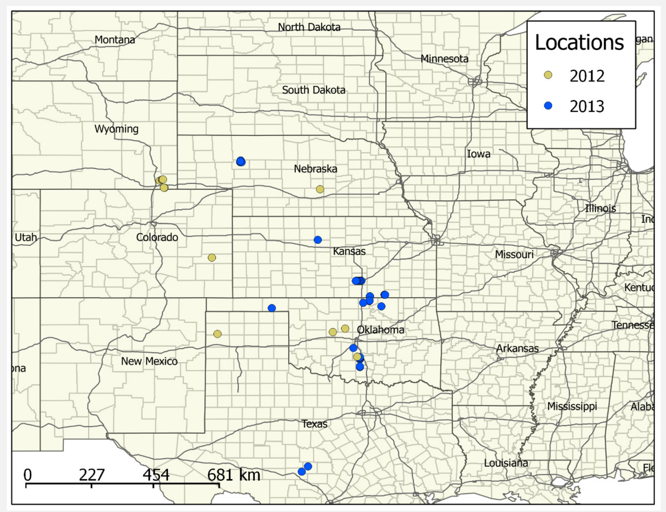

Figure 5. Map of all measurement locations for 2012 (yellow) and 2013 (blue) sampled events

- Hailstones were placed into four individual classes: spheroidal, disk, conical, and unclassified (Figure 6). For a hailstone to be classified as a disk shape its dominant dimension (x_1) was greater than twice that of the measured secondary dimension (y). Unclassified stones were often those with large protuberances such that an effective oblateness could not be determined.

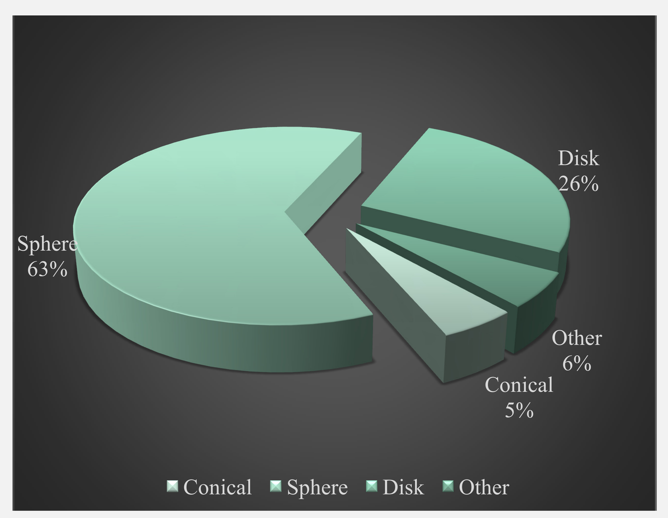

Figure 6. Hailstone shape classification distribution for 2012-2013 field observations.

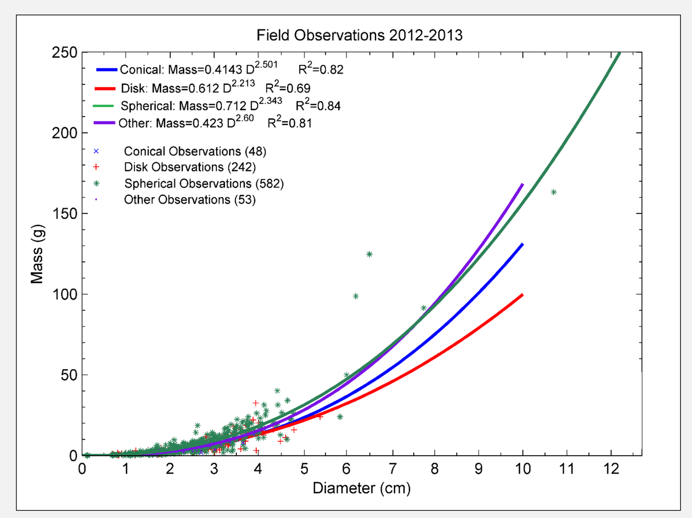

Figure 7. Observed mass shown as a function of equivalent diameter for each shape classification. Power-law fits shown for each class.

- The relationship between diameter and mass was examined with respect to the four shape classifications. A power-law fit was effective in describing the relationship as shown in Figure 7.
- Field observations were compared with laboratory ice spheres using tap and distilled water (in accordance with FM 4473) as shown in Figure 8. Test Ice spheres were made using spherical molds of 3.175 cm (1.25 in.), 4.445 cm (1.75 in), and 5.715 cm (2.25 in.).

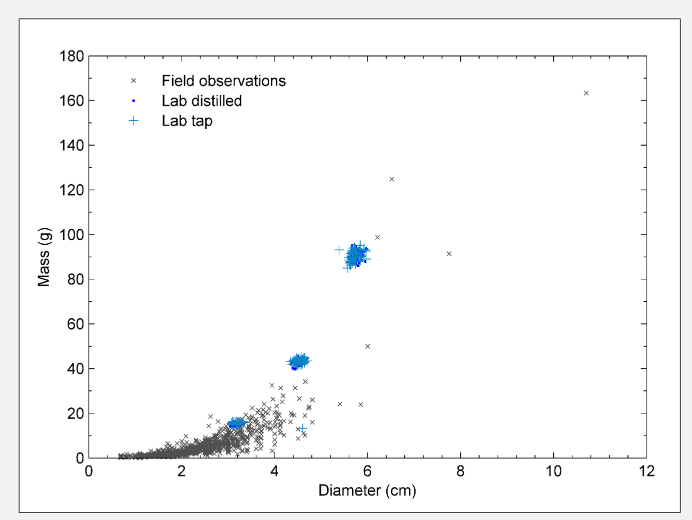

Figure 8. Measured mass shown as a function of equivalent diameter for measured hailstones (gray), laboratory tap (dark blue) and distilled water (light blue) ice spheres.

HARDNESS PROPERTY OF HAIL

- Compressive stress values ranged from 9.0×10^{-3} mPa to a maximum of 7.5 mPa. The mean value of the compressive stress distribution was 0.68 mPa. The probability distribution is shown in Figure 9.
- The largest compressive stress values were typically not associated with the largest diameter hailstones. Approximately 9% of the cataloged stones were too spongy or exhibited a ductile failure such that a peak compressive force could not be effectively determined.
- Laboratory ice spheres fell very close to the mean of that observed in the field (Figure 10). Field data were binned by equivalent diameter using 0.635 cm (0.25 in.) bin sizes for comparison with the three sizes of laboratory ice spheres.

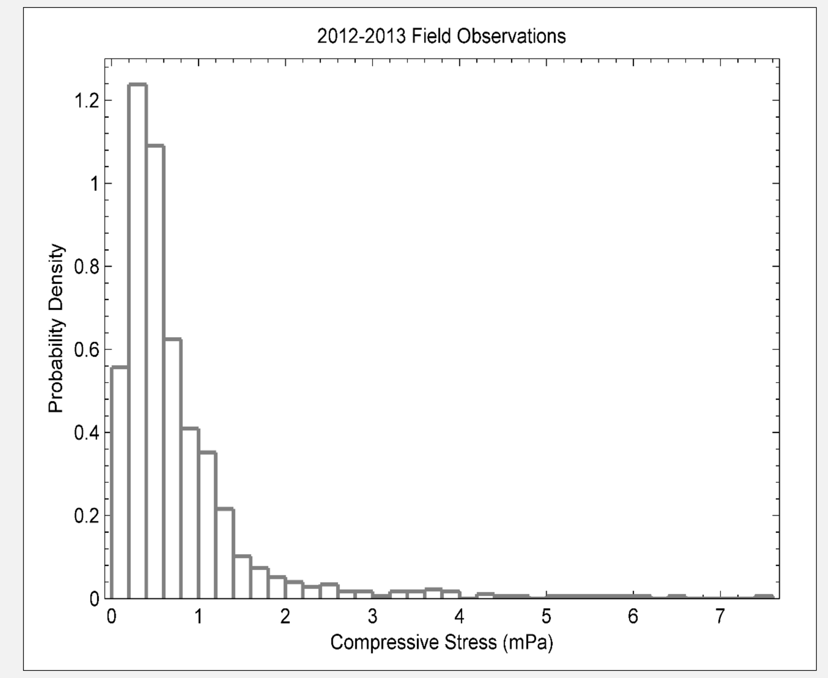

Figure 9. Probability distribution of compressive stress values found during the 2012 and 2013 field phases.

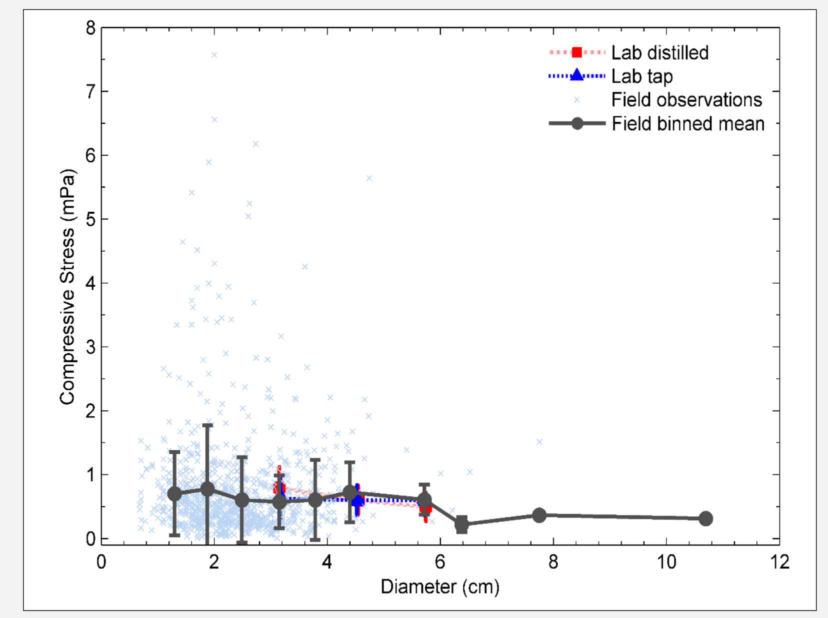

Figure 10. Compressive stress shown as a function of diameter for field observations (light blue), field observation groups (solid gray), laboratory tap water ice spheres (blue), and laboratory distilled water ice spheres (red). Error bars represent ±1 standard deviation from the mean for each group.

CONVECTIVE MODE

- Convective modes associated with each event were examined identify any correlation between hailstone characteristics and storm mode. The radar-based classification scheme presented by Smith et al. (2012) was used to classify each parent thunderstorm. The classification tree is shown in Figure 11.

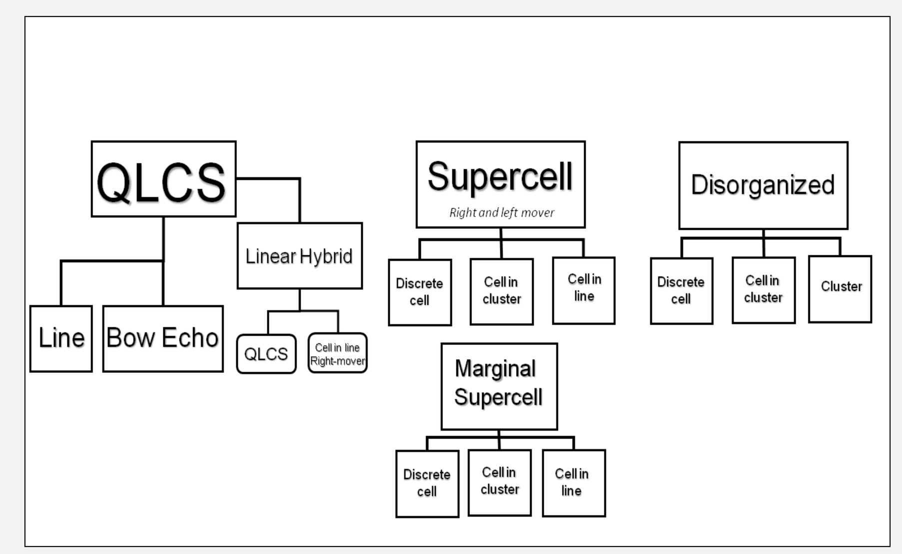

Figure 11. Primary and sub-classifications for the convective mode decision tree described by Smith et al. (2012).

- Additional scrutiny was applied for sub-classifications according to Smith et al. (2012). The characteristics for each major convective mode, excluding the sub-categories are provided in Table 2.

Table 2. Summary statistics for each primary convective mode classification.

Convective Mode	Events	Sample Size	Max Diameter (cm)	Mean Diameter (cm)	Max Compressive Stress (mPa)	Mean Compressive Stress (mPa)
QLCS	4	142	3.99	2.27	2.90	0.46
Supercell	19	746	10.69	2.41	6.46	0.76
Disorganized	2	33	3.12	1.87	7.46	1.53

Table 3 provides the summary statistics for each supercell sub-classification.

- A "supercell in a cluster – right mover" was the most common sub-classification with over 68% of hailstones from the complete dataset falling in this category.
- The single left moving-discrete supercell case produced the largest mean compressive stress value (1.6 mPa).
- The right moving-discrete supercell cases (4) exhibited the lowest mean compressive stress value (0.39 mPa) as shown in Figure 12.

For right moving supercells, the compressive stress values were typically clustered by parent updraft with small standard deviations. The sample size is too small to make any conclusions and it is unclear if the measurements collected by the field teams are truly representative of a random sample of the hail distribution.

Table 3. Summary statistics for supercell sub-classifications.

Sub-classification	Events	Sample Size	Max Diameter (cm)	Mean Diameter (cm)	Max Compressive Stress (mPa)	Mean Compressive Stress (mPa)
Discrete – RM	3	59	10.7	2.58	0.99	0.31
Discrete – LM	1	30	4.74	3.24	5.64	1.60
Cell in cluster - RM	7	514	7.75	2.37	7.57	0.79
Cell in cluster - LM	0	N/A	N/A	N/A	N/A	N/A
Cell in line - RM	0	N/A	N/A	N/A	N/A	N/A
Cell in line - LM	0	N/A	N/A	N/A	N/A	N/A
Marginal discrete	2	36	3.60	2.32	1.15	0.68
Marginal cell in cluster	4	107	3.77	2.13	6.18	0.66
Marginal cell in line	0	N/A	N/A	N/A	N/A	N/A

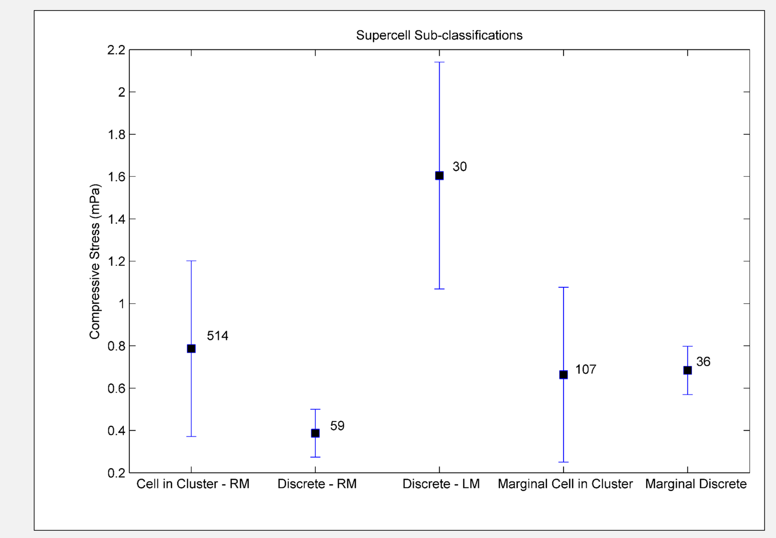

Figure 12. Mean compressive stress for each supercell sub-classification. Error bars represent ± 1 standard deviation from the mean. The sample size for each sub-classification is also provided.

SUMMARY

The data collected during the 2012 and 2013 IBHS field phases has provided a much needed baseline to evaluate the representativeness of existing laboratory test methodologies. The overall sample size from the two years of field measurement is miniscule compared to the number of hailstones a single thunderstorm can produce.

- Spheroidal shapes were the dominant type of hailstone encountered with a quarter of the dataset being disk-shaped. These two predominant shapes were observed in all parent thunderstorms. The typical size of stone measured during the two year field phase was approximately 2 cm with 60% of the dataset falling below the National Weather Service's severe threshold (2.54 cm / 1 in).
- Mean compressive stress values were generally similar to that found in laboratory testing of clear ice.
- Both hard and soft stones were encountered in most events. However discrete storm modes did exhibit some clustering of compressive stress values.
- The relationship between mass and diameter suggests a laboratory ice sphere of a given diameter will have a larger mass than a natural hailstone of equivalent diameter.
- The contribution of the hardness property of hailstones and how it relates to the imparted force and duration of impact is not as well understood. Future work will continue to focus on understanding this contribution and how common building materials perform in their new and aged states.

For references, please see the accompanying manuscript

***Acknowledgements**: The authors wish to thank the State Farm Insurance Technology Research And Innovation Laboratory (TRAIL) for personnel support during the 2013 field phase. Thanks are also extended to WeatherPredict Consulting Inc. for archival of observational and numerical model data during the 2012 and 2013 field phases.*

*Corresponding Author:
Ian Giammanco, Ph.D.
Email: igiammanco@ibhs.org
Insurance Institute for Business & Home Safety Research Center
5335 Richburg Rd, Richburg SC 29729